

CONCEPTUAL DESIGN OF A LONGITUDINAL HALO COLLIMATOR FOR J-PARC LINAC

Masanori Ikegami*, KEK, Tsukuba, Ibaraki 305-0801, Japan
 Tomohiro Ohkawa, JAERI, Tokai, Naka, Ibaraki 319-1195, Japan

Abstract

A longitudinal halo collimator has been designed for J-PARC linac. We plan to adopt a “successive collimation scheme” taking advantage of the three-fold symmetry of our arc section. Adopting this scheme, smaller momentum aperture of around 0.5 % can be achieved with larger physical horizontal aperture of the collimator. We are also expecting that this collimator system is effective in beam diagnosis in the beam commissioning.

INTRODUCTION

In J-PARC linac [1], the momentum spread at the RCS (Rapid Cycling Synchrotron) injection is required to be smaller than 0.2 % including the beam centroid jitter to enable momentum offset injection without substantial beam loss. While simulation studies show the present debuncher system is sufficient to meet this requirement [2, 3], we have concluded that it is preferable to have a longitudinal collimator for redundancy. The longitudinal collimator is also expected to be effective in preventing anomalous beams, arising from RF failure, from being injected into RCS. For these purposes, we plan to add a longitudinal collimation system in L3BT (Linac to 3-GeV RCS Beam Transport). The design consideration of the longitudinal collimator has been performed under limitations imposed by the magnet layout and tunnel geometry which have already been fixed [1].

CONCEPTUAL DESIGN

In a usual longitudinal collimator design, a single collimator is placed at a dispersion-peak of an achromatic arc section to remove particles with large momentum deviation [4]. There is a threshold of the momentum deviation, $\Delta p/p_{\max}$, above which all the particles are removed with the collimator, and the threshold characterizes the performance of the longitudinal collimation system. The threshold is characterized by the “separation ratio” $S = \eta_x / \sqrt{\beta_x}$, where η_x and β_x are, respectively, the dispersion function and horizontal beta function at the collimator location. In order to have a small threshold, it is required to make η_x large and β_x small at the same time, which imposes severe restrictions on the optics design of the arc section. Especially, excessively small β_x , or a narrow waist of a beam, often results in an increase of emittance growth.

To ease the restriction, we plan to adopt a new longitudinal collimation scheme of “successive collimation”. We have a 90-degree achromatic arc section in L3BT. The most distinctive feature of the arc section is its three-fold symmetry. Namely, it comprises three identical 30-degree achromatic sub-arcs or cells as shown in Fig. 1. We have a peak of dispersion function at the middle of each sub-arc, and the zero-current phase advance between two dispersion-peaks is around 270 degree. Instead of having single collimator at a dispersion-peak, we place three collimators with wider aperture at these three dispersion-peaks in series. At the first collimator, only the particles with certain momentum deviation and adequate betatron-phase are eliminated. For example, if a particle has a higher energy than the design value and betatron phase which makes the particle trajectory outside of the arc, it is likely to be eliminated. However, if the particle has the opposite betatron phase, it is unlikely to be removed. In other words, particles with undesirable betatron-phases survive the first collimator even if their momentum deviations are large. These surviving particles, however, will be eliminated with the second and the third collimators because of the phase advances between these collimator locations. In this “successive longitudinal collimation scheme”, smaller effective $\Delta p/p_{\max}$ is realized with smaller separation ratio with the help of betatron oscillation between the collimators. This scheme is advantageous in avoiding a narrow waist of a beam, which may result in an increase of emittance growth.

In a longitudinal collimator for negative hydrogen ion beams, eliminated particles are often charge-exchanged to protons and led to a dedicated beam dump [4]. However, this scheme requires elaborated design of a vacuum chamber for a bending magnet involving beam optics consider-

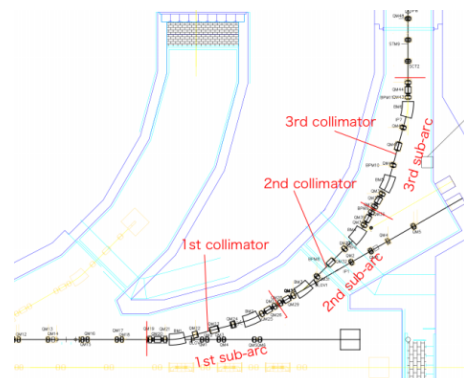


Figure 1: Layout of the achromatic arc section.

*masanori.ikegami@kek.jp

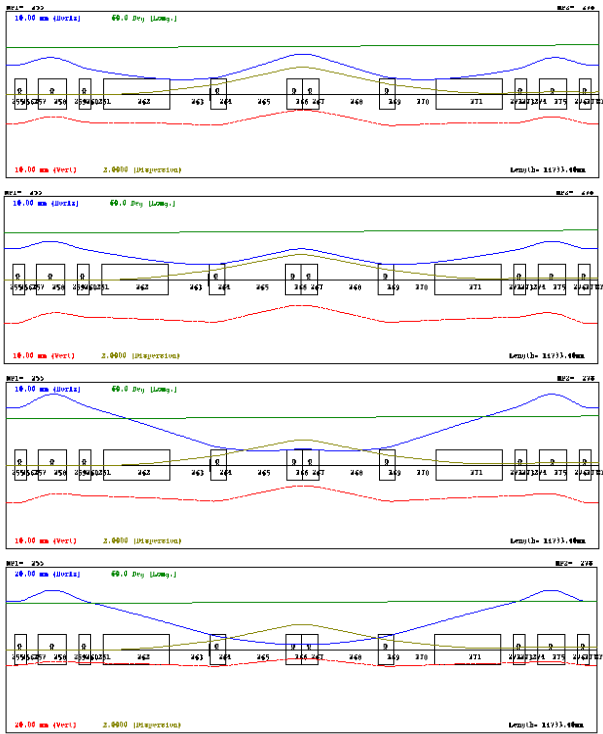


Figure 2: Beam envelope in a sub-arc. The blue and red lines, respectively, show the horizontal and vertical beam sizes. The brown line shows the dispersion function. The top: Case-I (the reference design), the second from the top: Case-II, the second from the bottom: Case-III, and the bottom: Case-IV. It should be noted that the scaling of the bottom figure is different from others.

ation of particle separation. The construction of an extra beam dump also imposes an economic burden. In our case, we plan to collect the discarded particles with an in-line absorber instead of delivering these particles to a dedicated dump. Detailed mechanical design of the collimator is now under way including the choice of absorber material. The radiation shielding is designed assuming the beam loss of 40W (0.12 % of the design beam power) in the arc section, and we expect that the amount of longitudinal halo is less than this limitation. This expectation is supported by particle simulations, where no visible longitudinal halo is observed [2, 3]. In addition, the limitation can be eased by adding local radiation-shielding around the longitudinal collimators. Needless to say, it is also possible to apply the charge-exchange dumping scheme to the successive collimation scheme in principle.

PARTICLE SIMULATION

The top figure in Fig. 2 (Case-I) shows the reference optics design for our arc section. We here consider three other optics designs for the arc section (Case-II to IV), in which the separation ratio is increased by adjusting quadrupole strengths. The beam envelopes for these designs are shown

Table 1: Main parameters at the dispersion maximum

Case	β_x [m]	η_x [m]	S [$m^{1/2}$]	$\Delta p/p_{\max}$ [%]
I	12.2	1.39	0.40	1.21
II	7.15	1.30	0.49	0.98
III	1.95	1.35	0.97	0.50
IV	0.79	1.57	1.76	0.31

in the rest of Fig. 2, and the characteristics of the optics designs are summarized in Table 1. In Case-II, the optics is modestly optimized to realize $\Delta p/p_{\max} < 1.0\%$, which is sufficient for anomalous beam elimination as discussed later. The optics is fully optimized in Case-III under the condition that we avoid the beam waist in the central focusing quadrupole. In Case-IV, the optics is aggressively optimized without the above condition. It should be noted that the beam has a waist in Case-IV in the middle of the central focusing quadrupole, whereas it has a small crest in Case-III. The design with larger separation factor is advantageous to have smaller momentum threshold, but it may be accompanied with larger emittance growth. It should be noted here that all four cases can be realized by adjusting quadrupole strengths without any magnet rearrangement and power supply upgrade.

To evaluate the performance of the successive longitudinal collimation, we have performed 3D particle simulations with PARMILA [5] from the exit of RFQ to the injection point to RCS. The peak current of 30 mA is assumed, and the initial distribution is generated with PARMTEQM [6]. Number of mesh points for space-charge calculation is set to $20 \times 20 \times 40$, and 95,322 simulation particles are employed. No error has been assumed. The strengths of the quadrupole magnets in DTL (Drift Tube Linac) and SDDL (Separate-type DTL) sections are determined to satisfy the equipartition condition. The collimator is modeled as a rectangular aperture without thickness, which is located 900 mm far from the dispersion maximum. We have a quadrupole magnet at the dispersion maximum, and the collimator location is 515 mm from its pole surface. This location is preliminarily selected to have enough space for possible local radiation shielding. The final position of longitudinal collimator will be determined with its detailed mechanical design. We have confirmed that this choice of collimator location hardly reduce the separation factor with the exception of Case-IV, where S becomes sensitive to the collimator location.

We need to find an optimum aperture width for the longitudinal collimators. The physical aperture should be determined not to scrape off the transverse halo. We have found that the minimum allowable physical aperture is around $19.5 \pi \text{ mm}\cdot\text{mrad}$. Then, we set the physical aperture, A_x , to be $23 \pi \text{ mm}\cdot\text{mrad}$ for all four cases. The $\Delta p/p_{\max}$ in Table 1 is obtained with a simple formula $\Delta p/p_{\max} = A_x/S$ assuming $A_x = 23 \pi \text{ mm}\cdot\text{mrad}$.

In particle simulations, we have confirmed that the rough

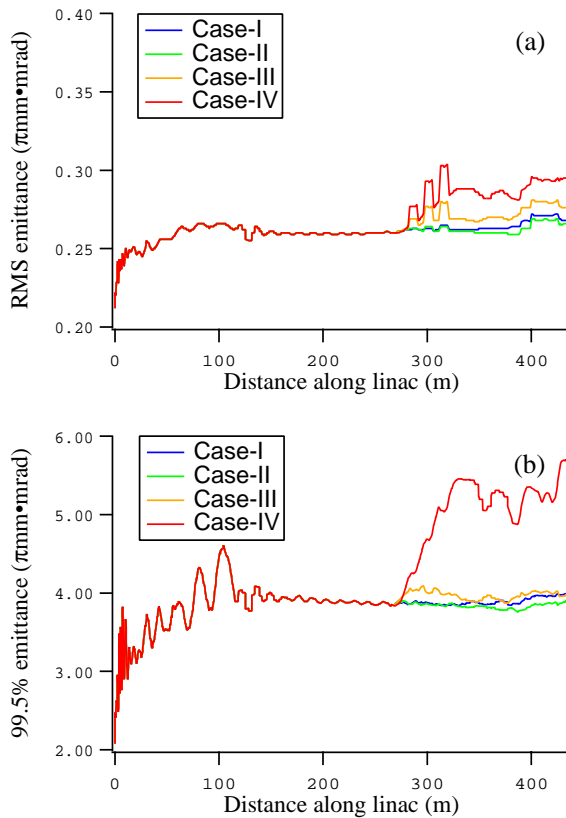


Figure 3: Emittance evolution in the linac and L3BT. (a) Horizontal rms emittance. (b) Horizontal 99.5 % emittance.

estimation of $\Delta p/p_{\max}$ with the above formula is accurate enough even with a rough adjustment of phase advance between collimators. We have found however substantial emittance growth in Case-IV as shown in Fig. 3. As clearly seen in Fig. 4, filamentation occurs in Case-IV possibly due to too narrow waist at the longitudinal collimator locations. It should be noted here that excess transverse emittance growth results in an increase of radiation load for the succeeding transverse halo collimators, which is limited to 2 kW.

These simulations indicates that the safely achievable $\Delta p/p_{\max}$ for this system lies around 0.5 %, while there may remain a room for further optimization. It is insufficient to ensure that the beams is in the momentum acceptance of the RCS. However, we expect that this collimator system is effective in dispersing the radiation load due to longitudinal halo at least. In addition, we can reduce $\Delta p/p_{\max}$, when occasion demands, by adding extra local shielding around the longitudinal collimator or tolerating additional radiation load for the transverse collimator. The simulation study shows that the anomalous beams arising from the RF failure of one of SDTL tanks will be eliminated if $\Delta p/p_{\max} < 1.0$ %. It means that Case-II is sufficient for this purpose.

Furthermore, we expect that this collimator system can

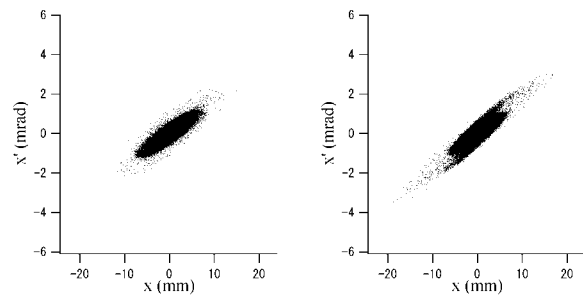


Figure 4: The phase-space distribution at RCS injection. Left: Case-III. Right: Case-IV.

be utilized for beam diagnosis. Namely, the physical aperture of the collimator, or $\Delta p/p_{\max}$, can be reduced in lower duty operation tolerating larger fractional losses at the collimator location. Then, comparing the beam losses in RCS with and without longitudinal collimation, we have information on how much beam loss can be attributed to the longitudinal halo. It is essentially important to identify the cause of beam loss in beam commissioning, and we believe that this collimator system can provide valuable information for improving of the beam tuning.

SUMMARY

Conceptual design of a longitudinal collimator for J-PARC linac has been performed. Adopting a “successive collimation” scheme, smaller momentum aperture has been achieved with larger physical horizontal acceptance of collimators. We expect that $\Delta p/p_{\max}$ of around 0.5 % can be safely achieved without significant increase of radiation load. There is a chance to achieve smaller $\Delta p/p_{\max}$ tolerating larger fractional loss at the longitudinal collimator or the downstream transverse collimator. The collimator system can also be utilized for beam diagnosis and is expected to provide a way of identifying the cause of uncontrolled beam loss.

REFERENCES

- [1] Y. Yamazaki ed., “Accelerator Technical Design Report for J-PARC”, KEK Report 2002-13, 2002.
- [2] T. Ohkawa, M. Ikegami, “Design of the Beam Transportation Line from the Linac to the 3-GeV RCS for the J-PARC”, EPAC 2004, Lucerne, 2004, p.1342.
- [3] M. Ikegami, T. Ohkawa, Y. Kondo, A. Ueno, “A Simulation Study on Error Effects in J-PARC Linac”, LINAC 2004, Lübeck, 2004, p.345.
- [4] N. Catalan-Lasheras, D. Raparia, “The Collimation System of the SNS Transport Lines”, PAC 2001, Chicago, 2001, p.3263.
- [5] H. Takeda, “PARMILA”, Los Alamos National Laboratory Report, LA-UR-98-4487, 1998.
- [6] Y. Kondo et.al., “Particle Distribution at the Exit of the J-PARC RFQ”, LINAC 2004, Lübeck, 2004, p.78.